Design and Fabrication of a Novel Microgripper Based on Electrostatic Actuation

J. Varona[1,2,3], E. Saenz[1,2], S. Fiscal-Woodhouse[2], A. A. Hamoui[3]
[1]*Universidad Panamericana-Bonaterra, Mexico*
[2] *Physical Design Center, Snowbush IP, Mexico*
[3]*Department of Electrical and Computer Engineering, McGill University, Canada*
varona@ieee.org

Abstract

This paper introduces a parallel-plate electrostatic microgripper fabricated in a standard surface micromachining technology. The simplicity of the design makes the gripper practical for a broad range of applications in biomedicine and microrobotics. Analytical models and experimental results are provided in support of the design.

1. Introduction

With the growing development of micro and nanotechnologies, there is a great demand for microtools suitable for manipulation of small-scale objects. Applications of mechanical mircotweezers are diverse and include equipment for microassembling of complex MEMS structures, biological microgrippers, microrobots for biomedical and aerospace applications, etc. [1, 2, 3]. Among the different actuating principles employed for the design of micromanipulators, the most popular are electrostatic, electrothermal, and shape memory alloys (SMA). Electrostatic actuators are the ones with the highest frequency response (up to hundreds of kHz under resonance) and the lowest power consumption, but their drawback is the need for relatively large voltages incompatible with typical CMOS electronic drivers. In the other hand, electrothermal actuators operate with low voltages and offer large output force but its applicability in microgrippers is limited due to the high power consumption and high operating temperatures that are unsuitable for biological and microrobotics uses. In turns, SMA technology like NiTi is based on a unique capability of reversible plastic deformation that allows the material to attaint certain shape when heated and then recover, fully or partially, its original shape when cooled down. However, SMA actuators suffer from the same limitations of electrothermal polysilicon devices in regards to high working temperatures and power consumption due to the required Joule heating. Furthermore SMAs are large in size with typical dimensions in the order of mm rather then μm, exhibit poor efficiency, and their displacement is hard to control [4].

The aim of this work is to develop a microgripper capable of clasping objects and particles smaller than 6-μm targeting portable biomedical and autonomous microrobotics applications. Accordingly, the electrostatic actuation has been chosen as the driving force due to the low power consumption and its functionality at room temperature.

2. Design Concept

Basically, a good microgripper must be able to firmly hold the object of interest with a force that is sufficiently high to keep it within the grips but at the same time sufficiently low to avoid damaging the material.

Traditional electrostatic microtweezers are based in the topology of the comb-drive actuator described in [5, 6]. The comb-drive consists of an array of interdigitated capacitor fingers where one set is fixed to the substrate and the other one has been released and is movable suspended with springs. In a typical comb-drive, the capacitance is linear with displacement and the driving force is assumed independent of the position of the moving fingers. While comb-drives are excellent for sensing applications like accelerometers, resonators and gyroscopes [7], their application as microtweezers presents some limitations. For instance, the comb-drive configuration demands the use of considerable area and requires some sort of mechanical transmission to couple the tweezers themselves. An example of the implementation of a comb-drive based microgripper is presented in [8] and depicted in Fig. 1.

978-1-4244-4480-9/09/$25.00 ©2009 IEEE

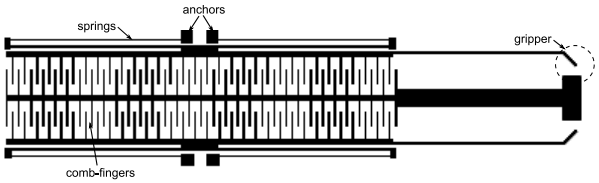

Figure 1. Typical comb-drive based microgripper actuator.

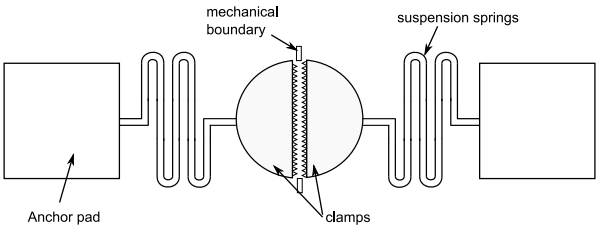

Figure 2. Proposed microgripper based in parallel-plate capacitance.

The microgripper design proposed in this work consists of two released polysilicon structures separated by a thin gap resembling the construction of a parallel plate capacitor. The two structures are supported by serpentine springs attached to an anchor pad in their far end. When a voltage difference is applied between the two structures, they will tend to collapse against each other due to electrostatic attraction thereby closing the gap. Objects located within the gap may be gripped in this manner by the clamping structures. The face of the structures is provided with triangular "teeth" along its length to ensure that the grabbed object is secured and it will not slip. The proposed microgripper design is sketched in Fig. 2.

This design offers a number of advantages over the classical electrostatic gripper based on comb-drive actuators. First, the gripper itself forms part of the actuator and no additional mechanical coupling transmission is needed. Second, the capacitance -and thus the driving force- increases with the displacement of the clamping structures so that lower voltages per unit area are required for closing the gripper in comparison to that of comb-drive actuators. Although stability and position control become more challenging, this is not an issue in a gripper application where only fully open/close states are of interest. Third, the microgripper design based on parallel plate capacitance can be more easily released from the substrate using flip-chip techniques [9] than comb-drive actuators and assembled onto other structures to realize more complex micromachines. For example, Fig. 3 shows how the microgripper could be released from its original substrate and attached to the tip of a probe to complete a micromanipulator. Other ideas for potential applications involve placing the gripper at the boundaries of a microchannel as to capture particles moving through a fluid, etc.

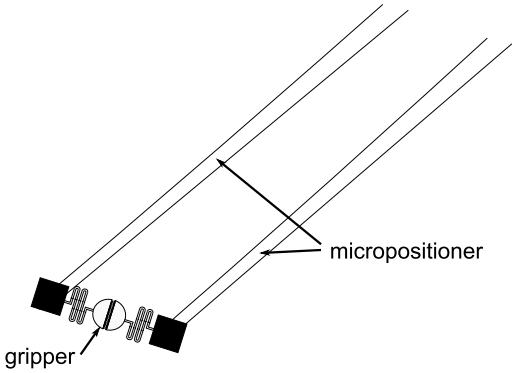

Figure 3. Application of gripper in a micromanipulator.

3. Analysis and Modeling

In the typical comb-drive actuator of Fig. 1, the driving force is attained by means of fringe fields from the comb fingers. Although the total capacitance increases linearly with displacement, the lateral capacitance that gets formed where the static and movable fingers overlap has a minimum contribution to the actuating force [10]. In such case, the fringe electric fields are assumed to be constant considering that the comb fingers are very large with respect to their displacement. Thus, the resulting actuating force is approximately fixed within a range of input voltages. This is a desirable property as a stable relationship between displacement and applied voltage is obtained over a wide range of x according to (1):

$$x = \frac{n\varepsilon V^2 t}{k_s g} \tag{1}$$

where n is the number of comb fingers, ε is the permittivity of the dielectric, V is the applied voltage, t refers to the thickness of the fingers, g is the gap between the comb fingers, and k_s is the spring constant of the system.

In contrast to the typical comb-drive actuator based on fringe capacitance and constant force, the electrostatic microgripper herein proposed and depicted in Fig. 2, employs the more direct parallel plate actuation method. Parallel plate actuators have been traditionally overlooked due to the instability of displacement as a function of input voltage. When voltage is applied, the electrostatic force between the

plates pulls them closer to each other but since the capacitance also increases with displacement, the attraction force grows geometrically and ultimately the plates tend to collapse. Therefore, the usable range for displacing the actuator's structures is limited to a fraction of the total gap between the plates in order to prevent them from collapsing. While this is certainly a problem in applications requiring precise position control, it is not of concern in the design of a microgripper that will be operated as a switch. Also, mechanical boundaries may be added to constrain the maximum displacement and keep the plates from touching one another as indicated in Fig. 2.

The model that represents a parallel plate electrostatic actuator is depicted in Fig. 4. The total capacitance between the plates is:

$$C = \varepsilon_o \varepsilon_r \frac{A}{d_o} \tag{2}$$

Where ε_o and ε_r are the permittivity of the free space and the relative permittivity of air, A is the area of the capacitor formed by the plates, and d_o represents the zero-voltage gap or gripper aperture.

The electrostatic force between the plates is given by:

$$F_e = \frac{1}{2}\frac{C}{d_o}V^2 \tag{3}$$

Let:

$$d = d_o - x \tag{4}$$

where x is the net displacement of the capacitor plates and d is the instantaneous gap or gripper aperture.

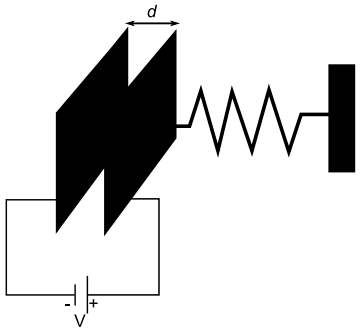

Figure 4. Model of a parallel-plate capacitor electrostatic actuator.

The electrostatic or actuating force as a function of the displacement x and the applied voltage is obtained by substituting (2) and (4) into (3):

$$F_e = \frac{1}{2}\varepsilon_o \varepsilon_r \frac{A}{d^2}V^2 \tag{5}$$

In turns, the mechanical restoring force due to the springs supporting the clamping plates is given by Hooke's law:

$$F_s = -k_s(d_o - d) \tag{6}$$

where k_s is the total spring constant of the system.

The state of stable equilibrium is achieved when F_e=-F_s. Though, as the input voltage is increased, the parallel plates are pulled closer to each other until they reach a "pull-in point" where the electrostatic force is too large and the plates simply collapse. This is, $F_e \to \infty$ when $d \to 0$. Therefore, the pull-in point represents the maximum displacement that can be achieved before the system becomes unstable and the plates collapse. The pull-in point may also be described as the minimum stable gap between the plates:

$$d_{\min} = d_o - x_{\max} \tag{7}$$

The pull-in point is reached when the electrostatic and spring reaction forces are tangential and equal in magnitude. Equating (5) and (6) and taking the derivative with respect to d yields:

$$\varepsilon_o \varepsilon_r \frac{A}{d^3}V^2 = k_s \tag{8}$$

Thus:

$$V^2 = \frac{k_s d^3}{\varepsilon_o \varepsilon_r A} \tag{9}$$

Now, substituting (9) into F_e=-F_s to find $d_{\min}$ gives:

$$d_{\min} = \frac{2}{3}d_o \tag{10}$$

The spring constant, k_s, is calculated based on the geometry of the spring. There are different types of spring designs that can be applied in MEMS actuators, some examples include crab-leg flexure, folded-beam flexure, Archimedean spirals, and serpentine springs

[11, 12]. The suspension springs should be designed to be flexible enough along the *x*-axis in the direction of the actuation, but rigid in the *y*-axis to oppose any potential movement in other direction. However, increasing the stiffness of the suspensions would require larger electrostatic forces and thus higher voltages to achieve the desired displacement.

For the microgripper design of this work, a curved serpentine spring was chosen as shown in Fig. 2. For design optimization, the analytical model of the spring constant is derived based on [13]. First, the serpentine spring is divided into segments as illustrated in Fig. 5 and the total spring constant is a combination of the bending stiffness of all the meanders. The total spring constant for one segment is approximated by:

$$k_{seg} = \frac{hG}{b^2\left(\frac{hG}{EI}b + 3a\right)} \tag{11}$$

where b is the length of the longitudinal or spam beam of the segment, a is the length of the horizontal or connector beam of the segment, I represents the bending moment of inertia for a rectangular beam, G is the shear modulus of elasticity for isotropic materials, E is the Young Modulus (162-GPa for polysilicon), and h is a shape factor constant.

The necessary parameters for calculating k_{seg} are estimated as:

$$I = \frac{tw^3}{12} \tag{12}$$

$$G = \frac{E}{2(1+\nu)} \tag{13}$$

$$h = tw^3\left[\frac{1}{3} - 0.21\frac{w}{t}\left(1 - \frac{w^4}{12t^4}\right)\right] \tag{14}$$

where ν is the Poisson's ratio for silicon (ν=0.3), w is the width, and t is the thickness of the beam.

Equation (10) is the spring constant of one segment; thus the total spring constant of the system, k_s, is obtained as the sum of N segments each of which is calculated using (10):

$$\frac{1}{k_s} = \sum_{n=1}^{N}\frac{1}{k_{seg(n)}} \tag{15}$$

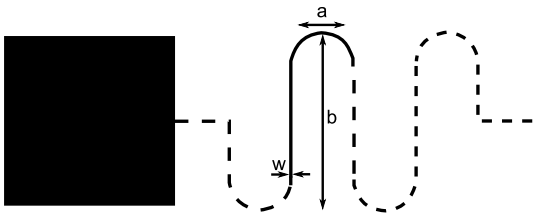

Figure 5. Serpentine spring model indicating the relevant geometrical parameters for one segment.

TABLE I. DIMENSIONS OF MICROGRIPPER ACTUATOR.

Geometry	Value
Zero-voltage gap or gripper aperture (d_o)	6-μm
Length of electrostatic plates (L_p)	100-μm
Thickness of electrostatic plates (t_p)	3.5-μm
Length of spam beams (b)	126-μm
Length of connector beams (a)	18-μm
Width of spring beams (w)	6-μm
Thickness of spring beams (t)	2-μm

A summary of the dimensions used for the design of the proposed electrostatic microgripper is given in Table I.

Using the geometric parameters from Table I and based on (9) and (4), the minimum voltage required for closing the gripper can be obtained. In this case, the pull-in point occurs when the gap between the plates is d_{min}=4μm, and the voltage required to close the microgripper is 63-V.

The results of the analysis for the operation of the parallel plate microgripper within the pull-in range are plotted in Fig. 6 and Fig. 7.

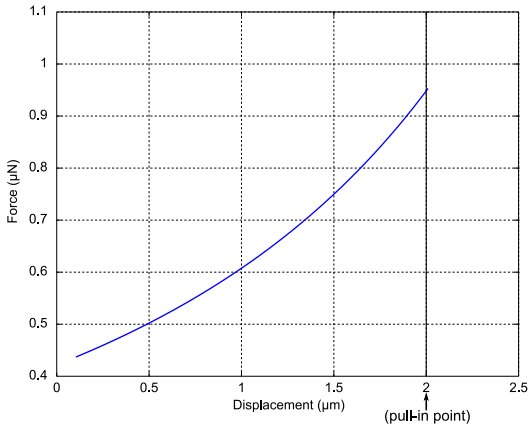

Figure 6. Variation of actuating force as a function of the displacement of the gripper plates within the pull-in range.

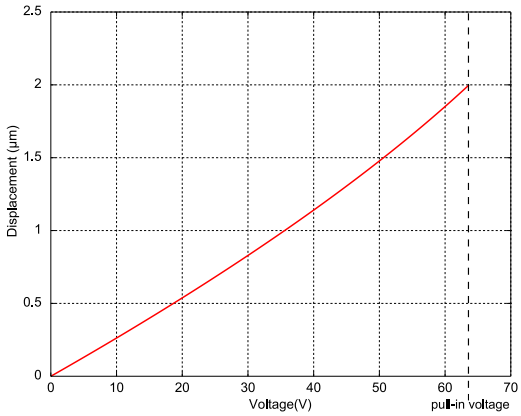

Figure 7. Displacement of the gripping plates versus voltage change within the pull-in range.

If the input voltage exceeds the pull-in value of 63-V the plates will collapse and the gripper will close.

4. Fabrication and Experimental Results

The microgripper presented in this paper was fabricated using the standard Multi-User MEMS Processes (MUMPs) [14]. MUMPs offers three layers of polysilicon and two sacrificial layers of phosphosilicate glass on an insulating film of silicon nitride. The last two polysilicon layers are releasable. A gold layer can be evaporated onto the surface at the end of the process by low pressure chemical vapor deposition. After construction, the sacrificial layers are removed in a bath of buffered HF acid.

The fabricated microgripper is shown in Fig. 8. To facilitate testing, the microchip was wire-bonded into a DIP-40 plastic package. A custom-made printed-circuit-board (PCB) including high-voltage buffers was used to control the input voltage applied to the actuator during the tests. A CCD camera mounted on a probe station was used to capture the displacement of the gripper. The experimental setup is presented in Fig. 9.

In the experiments, the voltage was swept incrementally to find the pull-in voltage. The obtained experimental results were compared to those predicted by the analytical model as shown in Fig 10.

Conveniently, the pull-in voltage was found to be about 27% lower than that estimated analytically. This deviation can be explained by the fact that the models used to calculate the spring constant do not account for the non-idealities of the fabrication process. Conventional models ignore the residual stress that is induced during fabrication of most microstructures and the localized deformation that occurs in coupling joint areas. In meander springs, the interaction of biaxial residual stress and loaded spring-plate coupling points is complex and accurate modeling is a challenging task. A comprehensive analysis of this phenomenon [15] shows that significant errors (of up to 100%) may result in predicting the pull-in behavior of electrostatic actuators when the spring constant is calculated using conventional models.

Thus, based on experimental data, a simple square signal with >46-V amplitude can be used to operate the electrostatic microgripper of Fig. 8.

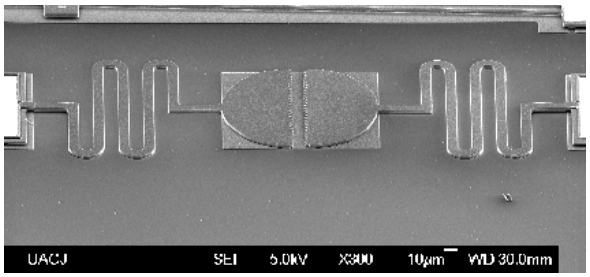

Figure 8. SEM micrograph of the fabricated microgripper.

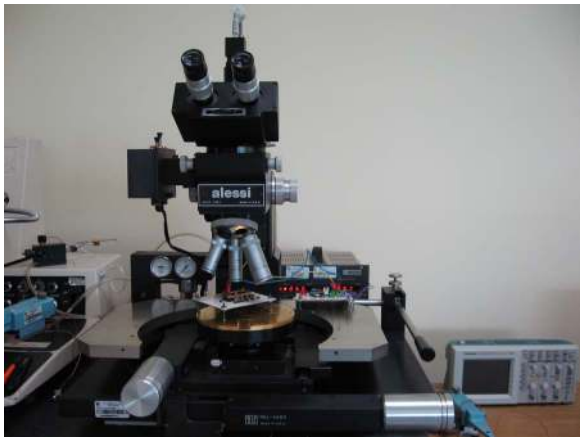

Figure 9. Test setup and equipment.

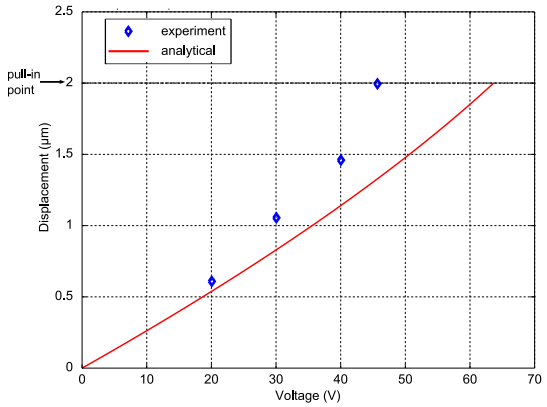

Figure 10. Comparison of experimental and analytical results.

5. Conclusions

A microgripper based on electrostatic parallel-plate actuation has been developed and tested. The parallel-plate configuration can be a good approach for realizing switching actuators where intermediate position control is not of concern. Parallel plate electrostatic actuators occupy a smaller area than that needed by a comb-drive design for a given output force and are more suitable for the typical post-processing and microassembling handling that is required in the realization of complex micromachines. The fabricated device requires just over 45-V for closing the gripper and it may find applications in microrobotic arms. A lower pull-in voltage could be achieved through optimization of the restoring springs.

6. Acknowledgment

This research was partially sponsored by the Instituto Panamericano de Alta Dirección de Empresas (IPADE) throughout the Center for Research and Innovation (CEPii).

Authors wish to thank Dr. Antonio Ramirez-Teviño from CINVESTAV and Dr. Jose Mireles Jr. from UACJ for providing access to laboratory and testing facilities.

7. References

[1] G. Greitmann and R. Buser, "Tactile microgripper for automated handling of microparts," 8th Intl. Conf. Solid-State Sensors and Actuators (Eurosensors IX), Stockholm, Sweden, pp. 372-375, 1995.

[2] C. J. Kim, A. P. Pisano, R. S. Muller, and M. G. Lim, "Polysilicon microgripper", in Tech. Dig. IEEE Solid-State Sensor and Actuator Workshop, pp. 48-51, 1990.

[3] P. Dario, M. Carrozza, C. Stefanini, Dapos, S. Attanasio, "A Mobile Microrobot Actuated by a New Electromagnetic Wobble Micromotor", IEEE/ASME Transactions on Mechatronics, Vol. 3, No. 1, pp.9-16, March 1998.

[4] R. Velazquez, E. Pissaloux, M. Hafez, and J. Szewczyk, "Measurement of SMA Thermal Properties in the Design/Evaluation of Actuators", 15th International Symposium on Measurement and Control in Robotics, Brussels, 2005.

[5] A. P. Pisano, "Resonant-structure micromotors," in Proc. IEEE Micro-Electro-Mechanical Systems Workshop, pp. 1–8, 1989.

[6] W.C. Tang, T.H. Nguyen, M.W. Judy, R.T. Howe, "Electrostatic-comb Drive of Lateral Polysilicon Resonators", J. Sensors and Actuators, Vol. A21-A23, pp. 328-331, 1990.

[7] R. T. Howe, R.S. Miller, K.J. Gabriel, W.S.N. Trimmer, "Silicon Micromechanics: Sensors and Actuators on Chip", IEEE Spectrum, pp. 29-35, July 1990.

[8] I.P.F. Harouche, C. Shafai, R. Gordon, "Design and simulation of a microtweezers using a controlled displacement comb drive", IEEE, pp. 341-343, 2006.

[9] D. Yan, A. Khajepour, R. Mansour, "Design and Modeling of a MEMS bidirectional vertical thermal actuator", J. Micromech. Microeng., Vol. 14, pp. 841–850, 2004.

[10] T. Kuendiger, G.M. Howard, P. Mokrian, M. Ahmadi, W.C. Miller, "Design and Analysis of Planar and Lattice Electrostatic Comb Drive Actuators", Proc. of IEEE-NEWCAS, pp. 19-22, 2005.

[11] R. Legtenberg, A.W. Groeneveld, M. Elwenspoek, "Comb-Drive Actuators for Large Displacements", J. Micromech. Microeng., Vol. 6, pp. 320-329, 1996.

[12] W.C. Tang, T.H. Nguyen, R.T. Howe, "Laterally Driven Polysilicon Resonant Microstructures", J. Sensors and Actuators, Vol. 20, pp. 25-32, 1989.

[13] H.A. Rouabah, C.O. Gollasch, M. Kraft, "Design and Optimisation of an Electrostatic MEMS Actuator with Low Spring constant for an 'Atom Chip'", Proc. NSTI Nanotech, Vol.3, pp. 489-492, May. 2005.

[14] J. Carter, et al., PolyMUMPS Design Handbook, MEMSCAP Inc., Revision 11.0, 2005.

[15] M. Lishchynska, N. Cordero, O. Slattery, C. O'Mahony, "Spring Constant Models for Analysis and Design of MEMS Plates on Straight or Meander Tethers", Sensor Letters Vol.4, No. 2, pp. 200-205, 2006.